DETACHED-EDDY SIMULATION OVER A REFERENCE AHMED CAR MODEL

Sagar Kapadia and Subrata Roy

Computational Plasma Dynamics Laboratory, Department of Mechanical Engineering
Kettering University, Flint, Michigan 48504, USA

kapa9202@kettering.edu, sroy@kettering.edu

Matthew Vallero

United States Air Force Academy, Department of Aeronautical Engineering
Colorado Springs, CO 80840, USA

Kenneth Wurtzler and James Forsythe

Cobalt Solutions, LLC
Springfield, OH 45504, USA

wurtzler@cobaltcfd.com, forsythe@cobaltcfd.com

Abstract This paper presents a Spalart-Allmaras based Detached-Eddy Simulation (DES) of the Ahmed reference car model with $25°$ and $35°$ slant angles using unstructured grids and the solver *Cobalt*. Comparisons are made to experimental laser doppler velocity measurements as well as total and surface pressure integrated drag. The Reynolds number based on body length was 2.78×10^6, making the boundary layers approaching the slant fully turbulent. The flow over the base slant in the experiments is attached at $25°$ and separated at $35°$. This causes a large drop in the drag with the increased slant angle as the vortices on the side of the slant are weakened due to the separation. These cases stress turbulence models due to the need to accurately predict the boundary layer separation over the slant as well as predict the pressures in the massively separated base region accurately. The DES results are compared to the experiments as well as the Spalart-Allmaras RANS model. DES is seen to predict separation at $25°$ slant angle, in contrast to the experiments. Drag is relatively close to the experiments, but the distribution of drag is more on the rear than on the slant due to the separation. At the $35°$ slant angle, DES is in good agreement to the experimental drag, with the correct distribution, while RANS over-predicts the drag.

Keywords: Turbulence simulation and modeling, hybrid methods, high Reynolds numbers, Automotive Aerodynamics

1. Introduction

Numerical simulation of the flow around complex configurations offers a powerful tool for analysis, e.g., a means to screen configurations prior to costly and time-consuming ground based tests. One example is automobile design in which Computational Fluid Dynamics (CFD) could be used to provide detailed information on performance (drag and downforce) as well as acoustics. Prediction of car aerodynamics has greatly challenged CFD because of the highly turbulent massively separated flow behind automobiles.

Most current engineering approaches, even to the prediction of unsteady flows, are based on solution of the Reynolds-averaged Navier-Stokes (RANS) equations. The turbulence models employed in RANS methods, at first sight, parameterize the entire spectrum of turbulent motions. While often adequate in steady flows with no regions of flow reversal, or possibly exhibiting shallow separations, it appears inevitable that RANS turbulence models will be unable to accurately predict the phenomena dominating flows characterized by massive separations.

To overcome the deficiencies of RANS models for predicting massively separated flows, Spalart *et al.* (1997) proposed Detached-Eddy Simulation (DES) with the objective of developing a numerically feasible and accurate approach combining the most favorable elements of RANS models and Large Eddy Simulation (LES). The primary advantage of DES is that it can be applied at high Reynolds numbers (as can Reynolds-averaged techniques) but also resolves geometry-dependent, unsteady three-dimensional turbulent motions as in LES.

This paper presents a Spalart-Allmaras based DES calculation of the Ahmed reference car model with 25° and 35° base slant angle using unstructured grids and the commercial unstructured solver *Cobalt*. Comparisons are made to the experiments of Lienhart *et al.* (2003) who made detailed off body measurements using LDA. Also total drag, as well as integrated pressure drag by component (slant, rear, front) are compared against the experiments of Ahmed *et al.* (1984). The Reynolds number based on body length was 2.78×10^6, making the boundary layers approaching the slant fully turbulent. The flow over the base slant in the experiments is attached at 25° and separated at 35°. This causes a large drop in the drag with the increased slant angle as the vortices on the side of the slant are weakened due to the separation.

2. Detached-Eddy Simulation

The base model employed in the majority of DES applications to date is the Spalart-Allmaras one-equation model (Spalart and Allmaras 1994, referred to as "S-A" throughout). The S-A model contains a destruction term for its eddy viscosity $\tilde{\nu}$ which is proportional to $(\tilde{\nu}/d)^2$, where d is the distance to the wall. When balanced with the production term, this term adjusts the eddy viscosity to scale with the local deformation rate S and d: $\tilde{\nu} \propto Sd^2$. A subgrid-scale model within the S-A formulation can then be obtained by replacing d with a length scale Δ directly proportional to the grid spacing.

To obtain the model used in the DES formulation, the length scale of the S-A destruction term is modified to be the minimum of the distance to the closest wall and a lengthscale proportional to the local grid spacing, i.e.,$\tilde{d} \equiv \min(d, C_{DES}\Delta)$. In RANS predictions of high Reynolds number flows the wall-parallel (streamwise and spanwise) spacings are typically the order of the boundary layer thickness and larger than the wall-normal spacing. Choosing the lengthscale Δ for DES based on the largest local grid spacing (i.e., one of the wall-parallel directions) then ensures that RANS treatment is retained within the boundary layer. Numerous applications have been performed using the current code [6] as well has a higher-order structured chimera code [7].

While a natural choice, and an aspect of nearly all hybrid methods, incorporating the grid spacing into the model can lead to inaccuracies as a DES grid is refined [5]. In boundary layers, as the grid spacing in the wall-parallel directions becomes smaller than about half of the boundary-layer thickness, the DES limiter reduces the eddy viscosity below its RANS level, though without allowing LES behavior. The resulting solution creates insufficient total Reynolds stresses, and can result in under-prediction of skin friction or early separation. Making the model more robust for these situations is currently being researched.

3. Calculation Details

The geometry used is depicted in [2] and shown in Figure 1. The body length (L) was 1044 mm. The grids for both slant angles were comprised of stretched prisms near the body, and tetrahedra elsewhere. The posts were included in both grids, although they were not included in the drag coefficient, just as in the experiments. The origin of the coordinate system was taken on the intersection of the symmetry and ground planes and level with the rear of the vehicle. The x-axis ran down the body, while the z-axis ran up. The posts were 50 mm tall, putting the bottom of the vehicle at z=50mm.

The $25°$ slant angle grid is pictured in Figure 1(a), and was created using the commercial program *Gridgen*. The grid contained 4.6×10^6 cells for the full geometry (both left and right sides), with clustering in a block surrounding the body. For the RANS calculation, a half body grid was used (2.3×10^6 cells), and symmetry assumed. The average y^+ for the first cell off the wall was < 0.3, with a geometric stretching factor of 1.3. The $35°$ slant angle grid is pictured in Figure 1(b), and was created using *VGRIDns* [3]. The grid contained 3.1×10^6 cells for the full geometry (both left and right sides), with clustering in a block surrounding the body. The RANS calculations were also done on the full

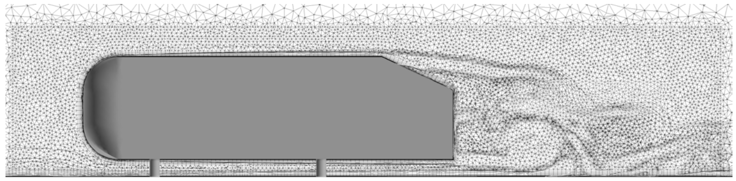

(a) $25°$ slant angle

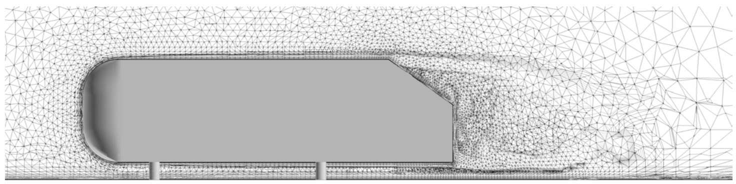

(b) $35°$ slant angle

Figure 1. Images of the grid in the symmetry plane, with countours of vorticity for an instantaneous DES solution.

geometry (i.e. symmetry was not assumed). The average y^+ for the first cell off the wall was < 0.3, with a geometric stretching factor of 1.3. Also shown in Figure 1 are contours of vorticity for the DES calculations showing evidence of LES content.

Boundary conditions were chosen to mimic the 3/4 open wind tunnel [2]. That is, the ground plane and the vehicle were set to no-slip, while the remaining boundaries were set to a far-field boundary condition. The extent of the ground plane upstream was chosen to give the correct boundary layer thickness assuming an empirical boundary layer growth. The resulting boundary layer was slightly thicker than the experiments at x=-1444mm; at y=30mm, the CFD velocity was 92% of freestream rather than 99%. The boundaries were about $\pm 6L$ upstream and downstream, $4L$ high, and $\pm 6L$ from the symmetry plane. The freestream velocity was set to 40 m/s, with $Re_L = 2.78 \times 10^6$.

RANS calculations were performed using a specified minimum global CFL of 1×10^6, and marched to a steady solution. DES calculations used a timestep of $7.2 \times 10^{-5} sec$, resulting in a non-dimensional timestep of 0.01 when non-dimensionalised by body height and freestream velocity. Initial transient from the DES were removed (first 2700 iterations), and time averages taken over an additional 6500 iterations, based on examining the convergence of a running time average of drag.

4. Results

For the 25° slant angle, Figure 2 depicts velocity vectors and contours of streamwise velocity for the simulations compared to the experiments at x=0mm, at the back of the vehicles. The strong side vortices in the experiments are clearly seen. Figure 2(a) compares S-A RANS to the experiments. The computed vortices are weaker, potentially because of the turbulence model and/or grid resolution. Although not shown, the S-A RANS separated at the beginning of the slant, but reattached prior to the back of the vehicle, just as in the experiments. The boundary layer thickens more along the centerline for the experiments than the computations, however. This could be due to a weaker adverse pressure gradient in the computations due to lower pressures on the rear (see drag results in Table 1).

S-A DES results are next shown in Figure 2(b). The flow is seen to separate with a large region of reverse velocity and weak vortices at the rear of the vehicle. Since DES would be expected to give lower eddy viscosity it is unlikely that the vortex is weaker due to the model. Instead it is presumed that the model has weakened the boundary layer, allowing it to separate, in turn weakening the vortices. The experimental boundary layer profile is almost 100mm thick at the rear because it is on the verge of separating. This places the RANS/LES interface deep into the boundary layer for this case, which weakens the turbulence model, as previously discussed.

To examine this effect, a calculation was performed where RANS was maintained prior to the back of the vehicle (i.e. $\tilde{d} = d$ for $x < 0$), and DES after the back of the vehicle (S-A DES-MOD – see Figure 2(c)). Although the situation improved, with a more shallow separation, the problem was not completely fixed. The presence of separation is probably due to different pressure gradients between the RANS calculations and this calculation due to differences in pressure on the back end.

The resulting drag coefficients are shown in Table 1. The drag on the slant, rear, and front is pressure drag only, for both the experiments and computations. Although DES agrees most closely to the experiments for the total drag, it is likely due to compensating errors. The drag on the slant is under-predicted due to the separation. RANS gives a reasonable prediction for the slant drag, due to predicting attached flow, but over-predicts the drag on the rear. Overall, none of the simulations are very satisfying.

The 35° slant angle case is examined next in Figure 3 by looking at velocity vectors and contours on the symmetry plane, since the flow at this angle is fairly two-dimensional with respect to the span in the experiments and computations. Since there were no measurement close to the body, the contours should be ignored close to the body for the experimental plot (Figure 3(a)). For the RANS results (Figure 3(b)), the velocity profile on the slant just prior

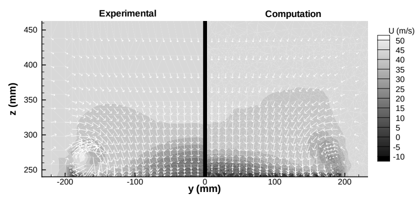

(a) S-A RANS

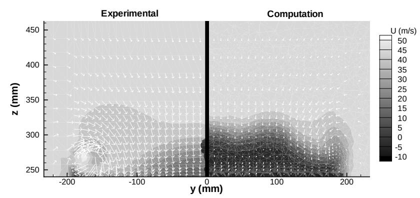

(b) S-A DES

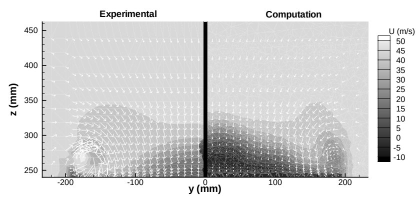

(c) S-A DES-MOD

Figure 2. Time-averaged velocity vectors and streamwise velocity contours at x=0mm, experimental [2] vs. computed.

Model	Slant	Rear	Front	Viscous	Total
S-A DES	0.084	0.127	0.027	0.042	0.281
S-A DES-MOD	0.106	0.104	0.028	0.044	0.283
S-A RANS	0.137	0.127	0.029	0.045	0.338
Exp[1]	0.145	0.077	0.019	0.057	0.298

Table 1. Drag Coefficients on the Ahmed body with 25° slant angle

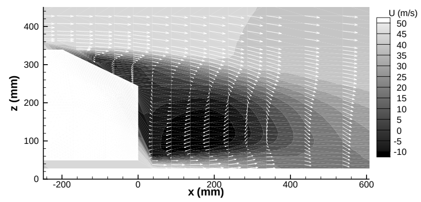

(a) Experiment

Model	Slant	Rear	Front	Viscous	Total
S-A DES	0.087	0.095	0.029	0.041	0.252
S-A RANS	0.130	0.115	0.031	0.044	0.319
Exp[1]	0.097	0.090	0.015	0.055	0.257

Table 2. Drag Coefficients on the Ahmed body with 35° slant angle

stress turbulence models due to the need to accurately predict the boundary layer separation over the slant as well as predict the pressures in the massively separated base region accurately. Cases on the verge of separating (or mildly separated and reattached like the 25° case) continue to pose strong challenges to predictive methods. Small differences in separation prediction (and possibly reattachment) may lead to apparently substantial differences as observed in the present case at 25°. At the 35° slant angle, DES is in good agreement to the experimental drag, with the correct distribution, while RANS over-predicts the drag. DES also accurately predicted the wake behind the 35° slant angle.

Acknowledgments

The authors would like to gratefully acknowledge the help of Dr. Michael Strelets who shared his group's unpublished Ahmed DES results and Prof. Kyle Squires for reviewing this manuscript.

References

[1] Ahmed, S.R., Ramm, G., and Faltin, G., "Some Salient Features of the Time-Averaged Ground Vehicle Wake," SAE 840300, 1984.

[2] Lienhart, H. and Becker, S., "Flow and Turbulence in the wake of a simplified car model," SAE Technical Paper Series, 2003-01-0656. Reprinted from: Vehicle Aerodynamics 2003 (SP-1786), 2003 SAE World Congress, Detroit, Michigan, March 3-6, 2003.

[3] Pirzadeh, S., 1996, "Three-dimensional Unstructured Viscous Grids by the Advancing Layers Method," *AIAA Journal*, **34**, pp. 43-49.

[4] Spalart, P.R. and Allmaras, S.R., 1994, "A One-Equation Turbulence Model for Aerodynamic Flows," *La Recherche Aerospatiale* **1**, pp. 5-21.

[5] Spalart P.R., Jou W.H., Strelets M., Allmaras S.R.: *Comments on the feasibility of LES for wings, and on a hybrid RANS/LES approach*, 1st AFOSR Int. Conf. on DNS/LES, Aug. 4-8, 1997, Ruston, LA. In: Advances in DNS/LES, C. Liu and Z. Liu Eds., Greyden Press, Columbus, OH, USA (1997).

[6] Squires, K.D., Forsythe, J.R., Morton, S.A., Strang, W.Z., Wurtzler, K.E., Tomaro, R.F., Grismer, M.J. and Spalart, P.R., "Progress on Detached-Eddy Simulation of massively separated flows", *AIAA 02-1021*, January 2002.

[7] Strelets M., *Detached eddy simulation of massively separated flows*, AIAA-2001-0879, 2001.